

THIS FILE COPY 880190C

Unclassified
SECURITY CLASSIFICATION OF THIS PAGE

REPORT DOCUMENTATION PAGE

Form Approved
OMB No. 0704-0188

3. REPORT SECURITY CLASSIFICATION AD-A208 615		1b. RESTRICTIVE MARKINGS	
3. DISTRIBUTION/AVAILABILITY OF REPORT Approved for public release, distribution unlimited.		5. MONITORING ORGANIZATION REPORT NUMBER(S) AFATL-TP-89-12	
a. NAME OF PERFORMING ORGANIZATION Instrumentation Technology Branch Advanced Guidance Division		6b. OFFICE SYMBOL (If applicable) AFATL/AGI	
7a. NAME OF MONITORING ORGANIZATION Instrumentation Technology Branch Advanced Guidance Division		7b. ADDRESS (City, State, and ZIP Code) Air Force Armament Laboratory Eglin Air Force Base, Florida 32542-5434	
c. ADDRESS (City, State, and ZIP Code) Air Force Armament Laboratory Eglin Air Force Base, FL 32542-5434		7b. ADDRESS (City, State, and ZIP Code) Air Force Armament Laboratory Eglin Air Force Base, Florida 32542-5434	
a. NAME OF FUNDING/SPONSORING ORGANIZATION Instrumentation Technology Branch/Advanced Guidance Div		8b. OFFICE SYMBOL (If applicable) AFATL/AGI	
c. ADDRESS (City, State, and ZIP Code) Air Force Armament Laboratory Eglin Air Force Base, Florida 32542-5434		9. PROCUREMENT INSTRUMENT IDENTIFICATION NUMBER	
10. SOURCE OF FUNDING NUMBERS		10. SOURCE OF FUNDING NUMBERS	
PROGRAM ELEMENT NO. 62602F		PROJECT NO. 2068	
TASK NO. 08		WORK UNIT ACCESSION NO. 20	
1. TITLE (Include Security Classification) Transducer Development for Explosive Measurements			
2. PERSONAL AUTHOR(S) David B. Watts and Michael T. Van Tassel			
3a. TYPE OF REPORT Paper		13b. TIME COVERED FROM Mar 87 TO May 89	
14. DATE OF REPORT (Year, Month, Day) May 1989		15. PAGE COUNT 19	
6. SUPPLEMENTARY NOTATION			
7. COSATI CODES		18. SUBJECT TERMS (Continue on reverse if necessary and identify by block number)	
FIELD	GROUP	SUB-GROUP	
19	01		
19	09		
9. ABSTRACT (Continue on reverse if necessary and identify by block number)			
<p>The objective of this paper is to present an overview of recent efforts to develop new measurement techniques to improve high explosive munition diagnostics. The development of high explosive munitions requires an accurate measurement of weapon effectiveness. One of the main elements of weapon effectiveness testing is the measurement of the explosive blast pressure. Blast waves are characterized by parameters such as initial shock intensity (peak overpressure), duration of the blast wave, impulse (force-time product) per unit area, and time of arrival of the wave. The standard method of measuring these parameters is with the use of free air</p>			
20. DISTRIBUTION/AVAILABILITY OF ABSTRACT <input type="checkbox"/> UNCLASSIFIED/UNLIMITED <input checked="" type="checkbox"/> SAME AS RPT. <input type="checkbox"/> DTIC USERS		21. ABSTRACT SECURITY CLASSIFICATION Unclassified	
22a. NAME OF RESPONSIBLE INDIVIDUAL David B. Watts		22b. TELEPHONE (Include Area Code) (904) 882-5375	
		22c. OFFICE SYMBOL AFATL/AGI	

DD Form 1473, JUN 86

Previous editions are obsolete.

SECURITY CLASSIFICATION OF THIS PAGE
Unclassified

89 5 16 047

19. Abstract (Concluded)

blast pressure transducers. The present state-of-the-art transducers do not have the frequency response necessary to accurately characterize the blast wave. The transducers experience mechanical resonance which makes it impossible to correctly measure the peak overpressure and, in turn, induces errors in the impulse measurement. This paper describes recent efforts to develop transducers that have sufficient frequency response and resonant frequency to improve high explosive munitions measurements. New measurement techniques employing piezoelectric polymer films and fiber optics have potential bandwidths approaching the Gigahertz regime. Other measurement systems that are optically based also have frequency bandwidth capability that approach Gigahertz responses. Some recent developments in transducers for blast pressure measurements utilizing these methods are presented in this paper. Additionally, development of a small helium driven shock tube for laboratory experimentation of blast pressure sensors is reviewed.

Transducer Development For Explosive Measurements

Instrument Society of America - SECON
Pensacola, Florida
May 24, 1989

Presented by:

David B. Watts and Michael T. Van Tassel
U.S. Air Force Armament Laboratory
Eglin Air Force Base, Florida 32542-5434



Accession For	
NTIS CRA&I	<input checked="checked" type="checkbox"/>
DTIC TAB	<input type="checkbox"/>
Unannounced	<input type="checkbox"/>
Justification	
By	
Distribution /	
Availability Codes	
Dist	Avail and/or Special
A-1	-

MSD 40A 89-115

TRANSDUCER DEVELOPMENT FOR EXPLOSIVE MEASUREMENTS

D. B. Watts and M. T. Van Tassel
Instrumentation/Simulation Branch
Advanced Guidance Division
U.S. Air Force Armament Laboratory
Eglin Air Force Base, Florida 32542-5434

ABSTRACT

The objective of this paper is to present an overview of recent efforts to develop new measurement techniques to improve high explosive munition diagnostics. The development of high explosive munitions requires an accurate measurement of weapon effectiveness. One of the main elements of weapon effectiveness testing is the measurement of the explosive blast pressure. Blast waves are characterized by parameters such as initial shock intensity (peak overpressure), duration of the blast wave, impulse (force-time product) per unit area, and time of arrival of the wave. The standard method of measuring these parameters is with the use of free air blast pressure transducers. The present state-of-the-art transducers do not have the frequency response necessary to accurately characterize the blast wave. The transducers experience mechanical resonance which makes it impossible to correctly measure the peak overpressure and, in turn, induces errors in the impulse measurement. This paper describes recent efforts to develop transducers that have sufficient frequency response and resonant frequency to improve high explosive munitions measurements. New measurement techniques employing piezoelectric polymer films and fiber optics have potential bandwidths approaching the Gigahertz regime. Other measurement systems that are optically based also have frequency bandwidth capability that approach Gigahertz responses. Some recent developments in transducers for blast pressure measurements utilizing these methods are presented in this paper. Additionally, development of a small helium driven shock tube for laboratory experimentation of blast pressure sensors is reviewed.

INTRODUCTION

Weapon effectiveness testing is critical to the development of high explosive munitions. One main aspect of this testing is the accurate measurement of the explosive blast pressure. The blast wave generated in an explosion imposes a dynamic load on any target in its field. This dynamic load is characterized by a rapidly reached peak value (overpressure) which then decreases as the blast wave decays. The net effect of the load depends both on the nature of the blast wave and on the geometry and construction of the target.

The blast wave from an explosion damages a structure by causing it to deform; these deformations may range from trivial damage to complete destruction. Basic considerations of analytical mechanics indicate that the damage potential of an explosive blast wave depends, (1) on the force that it exerts on a target, (2) on how long the force is applied, and (3) on the ability of the target to withstand the blast effects. The pertinent damaging aspect of a blast wave thus involves both its peak overpressure and its duration (impulse per unit area).

The very first mechanical effect of an explosive blast is a forceful blow from the instantaneous pressure jump in its shock front. This is followed immediately by the crushing effect of blast overpressure (pressure above atmospheric) and a blast wind of super-hurricane velocity. These blast wave effects then decrease quasi-exponentially with time until the pressure reaches atmospheric (zero overpressure), after which there is a slight negative phase along with a reversed blast wind (see figure 1). Blast waves are characterized by the initial shock intensity (peak overpressure, mach number, or particle velocity), duration of the blast wave, and impulse (force-time product) per unit area for the pressure forces in the blast. Also of interest is the arrival of the shock front as it travels from the center of the explosion to the location of concern (Ref 1).

One common method of measuring the peak overpressure and impulse per unit area of a blast wave is by using free air blast pressure transducers. These transducers are typically piezoelectric (crystal and ceramic) or piezoresistive (strain gage) in nature and do not have the frequency response necessary to accurately measure the transient pressure phenomena. The transducers experience mechanical resonance which makes it impossible to correctly measure the peak overpressure and, in turn, induces errors in the impulse measurements. Several transducer development efforts were recently undertaken to find new innovative sensor technologies that can achieve sufficient frequency response and resonant frequency for high explosive munitions measurements.

PIEZOELECTRIC SENSORS

Piezoelectricity is "electric polarization produced by mechanical strain in crystals belonging to certain classes, the polarization being proportional to the strain and changing sign with it (Ref.2)." Piezoelectric pressure transducers that employ piezoelectric crystals or ceramics are limited in frequency response by their physical properties and geometries. Piezoelectric materials used for these types of sensors include crystalline quartz and synthetic ceramics such as lead titanate and barium zirconate.

The resonant frequency of these transducers is limited by the mechanical design of the sensor housing, the geometry of the sensing element, and the method by which the sensing element is interfaced to the sensor housing. Theoretically, piezoelectric elements should be capable of extremely high resonant frequencies, especially as the size of the piezoelectric element is made smaller. However, as the piezoelectric element becomes smaller, it can produce less charge at a given pressure. Since any charge produced must be shared between the capacitance of the element itself and the capacitance of attached cabling, output of the sensor at remote charge amplifiers falls as the sensor becomes smaller (Ref. 3 & 4).

Piezoelectric polymer film gages that produce charge when subjected to pressure have been under development for several years (Ref. 2). Several types of piezoelectric film material exists: nylon 3,5,7,11; polyvinylidene fluoride (PVF₂); and a co-polymer known as VF₂/VF₃. These materials are made piezoelectric by stretching the material and then polling it, that is, subjecting it to a slowly decaying intense electric field that realigns its molecules (Ref.5). Francois Bauer, a French physicist, has recently patented a method of polling sheets of piezoelectric film such that every gage cut from the sheet will exhibit the same response (Ref. 6). If the gage response is reproducible, all that is needed is to calibrate one gage and the response of the gages will be known.

In contrast to conventional crystalline and ceramic transducers, piezoelectric polymer films have very wide-band frequency characteristics and low Q (quality factor). The quality factor is defined as the ratio of the resonant frequency to the bandwidth. Hence, a low Q corresponds to a relatively large bandwidth. Piezoelectric film has been employed as a transducer at frequencies from DC up to GHz.

Piezoelectric polymer film has a flat frequency response over a wide range which is a consequence of the polymer's softness. This eliminates the self-ringing found in brittle materials. By varying the thickness of the film, the resonance can be brought down to low MHz for very thick films (1mm) and up to GHz for very thin films (1 μ m). The capacitance is high enough for effective use at high frequencies when the signal from the piezoelectric film element is fed to a low impedance instrument (Ref.2).

Piezoelectric polymer films such as PVF₂ also have pyroelectric properties. Pyroelectricity is electric polarization induced by thermal absorption in crystals, with the polarization being proportional to the thermal change (Ref. 2). The shock front generated by an explosion usually reaches the blast pressure sensor before the thermal pulse

arrives, provided the sensor is located at a sufficient distance from the explosive. Therefore, the temperature change in the piezoelectric film is due to shock heating of the sensor and not the thermal pulse of the explosive which occurs after the pressure is measured. This pyroelectric property of PVF₂ is important since adiabatic shock heating will occur in coincidence with the change in pressure it experiences. If the temperature changes in PVF₂ and its surroundings are identical, then there will be no heat transfer and the pyroelectric response will be due to adiabatic heating of the PVF₂ only.

Bur and Roth of National Bureau of Standards report that for this special case of adiabatic heating of PVF₂, the pyroelectric charge signal is approximately eight percent of the piezoelectric charge. In general, for pressure measurements in environments where the pressure pulse occurs much more rapidly than the thermal pulse, this approximation can be applied to the transducer signal. Pressure measurements with dynamic range up to several hundred megahertz can be corrected with the eight percent temperature compensation (Ref. 7). Piezoelectric film sensors have been used by the Air Force Armament Laboratory for time-of-arrival measurements of detonation waves in explosives, explosive blast pressure measurements, and determining dynamic soil stresses generated by blast loading (Ref. 8).

As previously stated, going to a higher resonant frequency requires that the piezoelectric element itself be made smaller in thickness and lateral dimension. Smaller size of the piezoelectric element implies less voltage and charge available to drive cabling and amplifiers. Thin film piezoelectric materials show promise for integration of charge amplifiers into a monolithic chip. Silicon technology is an obvious choice for the chip itself, since this technology is well developed.

Piezoelectric elements produced by the process of sputtering of thin films such as zinc oxide (ZnO) are highly compatible with silicon chip fabrication technology. ZnO is a ceramic which can withstand fairly high process temperatures. It has been extensively investigated by researchers at the University of California at Berkley for both piezoelectric and pyroelectric sensors fabricated using silicon technology (Ref. 4). Basic research is continuing at the university level in this technology area.

PIEZORESISTIVE SENSORS

Piezoresistive sensors usually consist of a diaphragm containing resistors in a wheatstone bridge configuration. Under the influence of a pressure difference across its thickness, the diaphragm flexes and places strain on the

resistors, which causes them to change resistance and produce an output voltage proportional to both the applied pressure and the bridge supply voltage. Because the diaphragm must be thinner than its supporting regions, it has the lowest resonant frequency of any component within the small sensor package, and consequently places the upper limit on the frequency response of the sensor.

The use of silicon as the substrate material as well as the diaphragm offers the advantages of batch fabrication techniques used for silicon technologies such as integrated circuits. Resistors can be diffused or implanted into the silicon diaphragm (see Figure 2). Additionally, signal conditioning electronics can be built into the silicon chip. The piezoresistive effect in silicon is direction dependent. Finite element modeling of various silicon diaphragm configurations on a silicon substrate indicate an upper resonant frequency limit in the range of 1-6 MHz. This limit is material dependent and could rise if some material (other than silicon) with a higher strength-to-weight ratio could be used. The resonant frequency limit may be too low for some explosive blast pressure measurements. Presently available piezoresistive silicon devices are thought to approach fundamental upper limits on resonant frequency (Ref. 4).

Semiconductor piezoresistive sensors do, however, offer high sensitivity, or gage factor, perhaps 100 times that of wire strain gages (Ref. 9). Gage factor is defined by the fractional change in resistance divided by the axial strain. The gage factor for semiconductor sensors is determined by the doping level, and it also varies as a function of temperature. Most materials, such as those used for wire and foil strain gages, have factors only slightly higher than 1.6. This suggests that there is a small change in the material resistivity with stress (Ref. 10).

Piezoresistive gages made of manganin are presently used for explosive measurements. Manganin gages are composed of a thin metal foil grid laminated to a plastic insulator similar to a strain gage. Typical manganin sensitivity is 0.0027 ohms/Kilobar. These gages are not made for resolution below 1 Kilobar. The gages are only accurate when forces run perpendicular to the gage face. To avoid gage heating manganin gages need to be activated using a pulsed power supply - applied just before pressure is experienced. Pulsed excitation can go as high as 300 volts with no gage heating due to the short times involved. Manganin gages have measured pressures up to 400 Kilobars. These gages are typically used to measure detonation pressures internal to the explosive (Ref. 11).

PHOTOELASTIC OPTICAL SENSOR

The photoelastic effect in transparent materials can be used to create an optical pressure sensor for explosive blast pressure measurements. This effect is due to the double refraction in transparent materials when a stress is applied. An explosive blast pressure wave subjects the photoelastic material to a uniaxial strain field that is perpendicular to the direction of light traveling through the material. When this stress is applied in the x direction the index of refraction (defined by Equation 1) increases along that direction, while the index of refraction along the y direction remains constant (see figure 3). This doubly refractive, or birefringent material, separates an incident beam of light into two diverging rays, known as ordinary and extraordinary rays. The extraordinary ray traveling along the x axis direction propagates at a slower speed than the ordinary ray traveling along the y direction. The index of refraction is defined as:

$$n = c/v \quad (1)$$

where:

n = the index of refraction

c = the velocity of light, 2.9×10^8 m/s

v = the velocity of light in the material

Consequently, the higher the index of refraction of a material the slower the velocity of the ray propagating through it becomes. Hence, the x axis is known as the slow axis and the y axis is known as the fast axis.

In Figure 3, unpolarized light is transmitted to the sensor by a multimode fiber. A GRIN (GRaded INDEX) lens collimates the light through a polarizer oriented at $\pi/4$ (45°) with respect to the x axis of the material. The polarizer blocks one of the components of light and transmits the other into the photoelastic material. The now linearly polarized light is changed to circularly polarized light by the quarter wave plate. If the material is not stressed, then the circularly polarized light will pass through unchanged. A prism polarizer then spatially separates the two polarization components yielding equal intensities. The orientation of the prism is chosen in order to analyze the light exiting the material at angles of $+\pi/4$ and $-\pi/4$ with respect to the fast and slow axes in the material. The two signals are then focused into two receiver fibers by two GRIN lens, for transmission into two photodetectors. The quarter wave plate is used for optical biasing. Because of the sine squared relationship between the stress birefringence and the transmitted intensities of the sensor's output channels (seen in Equations 2 & 3) the quarter wave plate results in the

sensor initially operating at the point of greatest sensitivity (the inflection point of the sine square curve). When the material is stressed, the polarized rays experience a phase shift. This phase shift is proportional to the magnitude of the applied stress and material thickness, and is referred to as stress induced birefringence.

With the sensor configured as in Figure 3, a change in the applied stress results in a change in optical transmission. This results in changed light intensities incident on the optical detectors. For this configuration, the output intensity for the $\pi/4$ and the $-\pi/4$ orientations is given by:

$$I_{\pi/4} = I \cdot \sin^2(\Gamma(S)/2 - \pi/4) \quad (2)$$

$$I_{-\pi/4} = I \cdot \sin^2(\Gamma(S)/2 + \pi/4) \quad (3)$$

where:

I = input optical intensity

$\Gamma(S)$ = stress induced birefringence

The induced birefringence in an isotropic photoelastic material as a function of the applied stress is given by:

$$\Gamma(S) = (2\pi t/f)S \quad (4)$$

where:

t = the optical path length

f = a material constant (psi/fringe/in)

s = the applied stress (psi)

Equation 4 shows that the stress induced birefringence, and therefore, the sensor sensing range and sensitivity are dependent on the material geometry

By using the identities:

$$\sin(A+B) = \sin A \cos B + \cos A \sin B$$

and

$$\sin(A-B) = \sin A \cos B - \cos A \sin B$$

and squaring the results, Equations 2 and 3 can also be shown in the following form:

$$I_{\pi/4} = I/2 - I \cdot \{\sin \Gamma(S)/2\} \cos \Gamma(S)/2 \quad (5)$$

$$I_{-\pi/4} = I/2 + I \cdot \{\sin \Gamma(S)/2\} \cos \Gamma(S)/2 \quad (6)$$

This allows the sum and difference of these two equations to be written as:

$$I_{sum} = I_{\pi/4} + I_{-\pi/4} = I. \quad (7)$$

$$I_{diff} = I_{-\pi/4} - I_{\pi/4} = 2I \cdot \{\sin \Gamma(S)/2\} \cos \Gamma(S)/2 \quad (8)$$

The sum-difference sensor output becomes:

$$\begin{aligned} \text{sum-difference} &= I_{diff}/I_{sum} = 2 \sin \Gamma(S)/2 \{\cos \Gamma(S)/2\} \\ \text{sum-difference} &= \sin \Gamma(S) \end{aligned} \quad (9)$$

Equation 9 shows that the sum-difference sensor output is intensity invariant. This provides immunity from source light intensity variations and optical fiber microbending losses.

The measurement bandwidth capability of a photoelastic pressure sensor is determined by the natural resonant frequency of the photoelastic sensing element and the speed of sound in the material.

The resonant frequency of a photoelastic sensing element is determined by the mechanical properties of the sensing element (Young's modulus and material density) and its geometry. For a rectangular parallelepiped loaded along its height (L), the natural resonant frequency is found to be:

$$f = n/2L(\sqrt{E/\rho}) \quad (10)$$

where:

f = the natural resonant frequency

n = an integer number

L = the height of the sensing element

E = Young's modulus

ρ = the material density

$\sqrt{E/\rho}$ = the acoustic velocity

As can be seen from Equation 10, the resonant frequency is dependent on the height of the sensing element, since the material properties of the photoelastic material are constants. By proper selection of the photoelastic material in conjunction with its height, resonant frequencies in the upper MHz region can be achieved. This resonant frequency is achieved independent of the sensor's pressure range, since the sensing range is defined by optical path length (refer to Equation 4).

The limitation in the measurement bandwidth capability of a photoelastic sensor with acoustic velocity results from the measured pressure propagating through the sensing element material at the speed of sound. The limitation depends on the speed of sound in the material and distance between where the pressure is applied and the location of the optical axis. The acoustic velocity of most optical glasses is sufficient to support frequencies into the megahertz.

Static loading experiments can be performed to determine the stress optical coefficient of photoelastic materials. This coefficient is used in defining the required geometry of a sensing element to achieve a desired pressure sensing range. The stress optic coefficient is a measure of the magnitude of induced birefringence of a material for a given load.

Sensing element material, substrate (sensor housing) material, and the method by which the sensing element is attached to the substrate material can all have an effect on both risetime and the coupling of resonances into the sensing element. Dynamic loading experiments may be used to determine the effect of the extent of these effects (Ref. 3).

Experimental results on resonant frequency, pressure range, and response time show that the photoelastic based sensor is well suited to the measurements of blast waves.

OPTICAL FABRY-PEROT RESONATOR PRESSURE SENSOR

A sensor based on a Fabry-Perot resonator has been investigated for the characterization of blast waves. A Fabry-Perot resonator is constructed of two partially reflecting surfaces parallel to one another so that light waves may bounce back and forth between them several times (Figure 4). Used as a laser resonator, only light of specific frequencies traveling perpendicular to the reflecting surfaces is reinforced by successive reflections and amplifications to form an oscillating mode. The optical characteristics of the resonator depend on these relative amplitudes and phases of these reflections. The phase Φ is defined as:

$$\Phi = 2\pi t/\lambda \quad (11)$$

where λ is the wavelength and t is the thickness of the cavity. It can be shown that the reflected spectrum is a series of peaks, each separated by a phase difference of π radians. Furthermore, the shape of the maxima and minima depends on the reflectivities of the two surfaces.

It can be seen from Equation 11 that the relative phase depends on both the cavity thickness and the wavelength. Therefore, for a fixed wavelength, the reflected intensity is a measure of the cavity thickness. By using a diaphragm as one reflector in the resonator, the sensor is optically measuring the diaphragm displacement.

The sensor is a combination of a micromachined silicon diaphragm and optical fiber assembly held in an aerodynamic housing. The gap between the diaphragm and the fiber end defines the resonant cavity.

Reflectivity of the sensor is measured at several wavelengths. By taking the ratio of the intensities of two measured wavelengths, it is possible to compensate for intensity variations in the optical system. The reflection characteristics are shown in Figure 5, with wavelength as a parameter. It can be seen that the curve is approximately sinusoidal with phase (or thickness).

It can be shown that taking the ratio of the two wavelengths allows any variable system losses to be compensated, as shown by Figure 6. The main problem with this compensation scheme is that the transfer characteristics are very nonlinear. Although the characteristics should be well defined analytically, they may vary from sensor to sensor due to differences in the fabrication process. Without further compensation, the manufacturing tolerances would have to be very tight to achieve acceptable accuracy.

A compensation system is an optoelectronic interface, shown in Figure 7. It contains a broadband LED and is used as the light source. This light is modulated by the sensor cavity and is returned to the interface unit, where it is separated into a number of spectral channels by a 5 channel wavelength division multiplexer (WDM). Two channels are coupled to high bandwidth detectors where their ratio is used to generate a normalized signal. The remaining channels are coupled to low bandwidth detectors and, in conjunction with high bandwidth signals, are used for calibration and linearization of the sensor head response.

Modeling of the Fabry-Perot optical resonator pressure sensor included numerical analysis of the optical system and finite element analysis of the mechanical design. Finite element modeling of silicon diaphragms was discussed earlier in this paper under piezoresistive sensors. As previously mentioned, the resonant frequency upper limit of the silicon diaphragm is in the range of 1-6 MHz. The predicted characteristics of resonant frequency and maximum pressure range show that the Fabry-Perot based sensor is suited to the measurements of blast waves (Ref. 4).

REMOTE BLAST PRESSURE SENSORS

A study was conducted to evaluate the feasibility of removing the pressure measuring sensors from a blast field, enabling a totally remote measurement of pressure time history. By removing the sensors from the blast field, the uncertainties introduced by fragments, shields protecting the sensors, and thermal effects would also be removed. It was thought that a laser based measurement technique would meet our objective. After an extensive survey of literature on laser probes, no reasonable technique for remote measurement of pressure-time history of blast waves was found.

The main difficulty is that the pressure pulse behind the blast wave is physically very short. This, together with the very weak interaction of laser photons with air molecules, leads to extremely weak signals. Another problem is the interference from the extreme brightness created by the explosion fireball. Lasers with a continuous output offer the possibility of making a continuous pressure versus time record, but pulsed lasers are needed to overcome the background interference. The use of pulsed lasers necessarily leads to snapshot measurements at the pulse repetition frequency (PRF), rather than a continuous history. Consequently, attention was turned to an alternative technique: measurement of the shock speed with a laser.

The peak pressure behind a shock in an ideal gas is directly related to velocity of the shock. This relationship is obtained from detailed calculations. Figure 8 shows this relationship. The speed of the shock wave is detected from the doppler shift of the reflected laser beam (Ref. 12).

The objective of measuring the blast pressure with no hardware embedded in the field was partially realized, although only the peak value at discrete points could be measured. This also permits measurements closer to the explosion than is possible with quartz gauges.

Shock Tube

A shock tube was developed for the non-destructive testing, characterization, and calibration of blast pressure gages. This device is capable of generating pressure pulses up to 200 psi of overpressure and rise times of less than 10 microseconds. The shock tube consists of a high pressure helium driver, diaphragm, expansion nozzle, and the barrel where the pulse develops and sweeps by or impinges on the test gage. The shock overpressure is variable by the operator's setting of initial driver pressure and the selection of a diaphragm with the proper burst pressure. Pressure gages placed in the shock tube will experience similar shock wave characteristics as it would if placed within an open air explosive blast field (Ref. 13).

This shock tube is an invaluable laboratory tool for the continuing evaluation of prototype pressure sensors.

SUMMARY

Present state-of-the-art transducers do not have the frequency response necessary to accurately characterize explosive blast waves. A review of the sensing range, bandwidth, and resonant frequency of several new explosive measurement techniques show that those based on piezoelectric polymer films and photoelastic optical sensors are the most promising. Both techniques offer wide sensing ranges with potential bandwidths approaching the Gigahertz regime.

REFERENCES

1. Kinney, Gilbert F., and Graham, Kenneth J., Explosive Shocks in Air, second edition, Springer-Verlag, New York, 1985, ISBN 0-387-15147-8.
2. Pennwalt Corporation, Philadelphia, PA, Kynar Piezo Film Technical Manual, 1983.
3. Ultrahigh Frequency Pressure Sensors - Geocenters, Inc., AFATL-TR-88-49, October 1988.
4. Ultrahigh Frequency Pressure Sensors - Novasensor, AFATL-TR-88-77, October 1988.
5. The Use of Commerical Piezofilms for Stress Wave Measurements, J. A. Charest and C. S. Lynch, Dynasen, Inc., 38th ARA meeting, Tokyo, Japan, October 1987.
6. Recent Development in Piezoelectric Polymer Stress Gauges, R. P. Reed, Sandia National Lab, RCC - 14th Transducer Workshop, Colorado Springs, CO June 1987.
7. A Polymer Pressure Gage for Dynamic Pressure Measurements, A. J. Bur and S. C. Roth, National Bureau of Standards, Proc. Second Symposium on the Interaction of Nonnuclear Munitions with Structures, Panama City, FL, April 1985.
8. Development of an NBS Polymer Gage for Dynamic Soil Stress Measurement, NBSIR 85-3135, April 1985.
9. Omega Engineering, Inc., Stamford, CT, Pressure and Strain Measurement Handbook and Encyclopedia, 1985.
10. Endevco Corporation, San Juan Capistrano, CA, Shock and Vibration Measurement Technology Short Course Text Book, 1987.
11. Use of Manganin Gages to Measure Sweeping Shock Pressure Loads, B. W. Duggin and R. I. Bulter, Sandia National Laboratories, ISA-70 Silver Jubilee International Conference and Exhibit, Philadelphia, PA, October 1970.
12. Remote Blast Pressure Sensor, AFATL-88-55, August 1988.
13. Portable High Explosive Pressure Transducer Calibration, AFATL-88-76, August 1988.

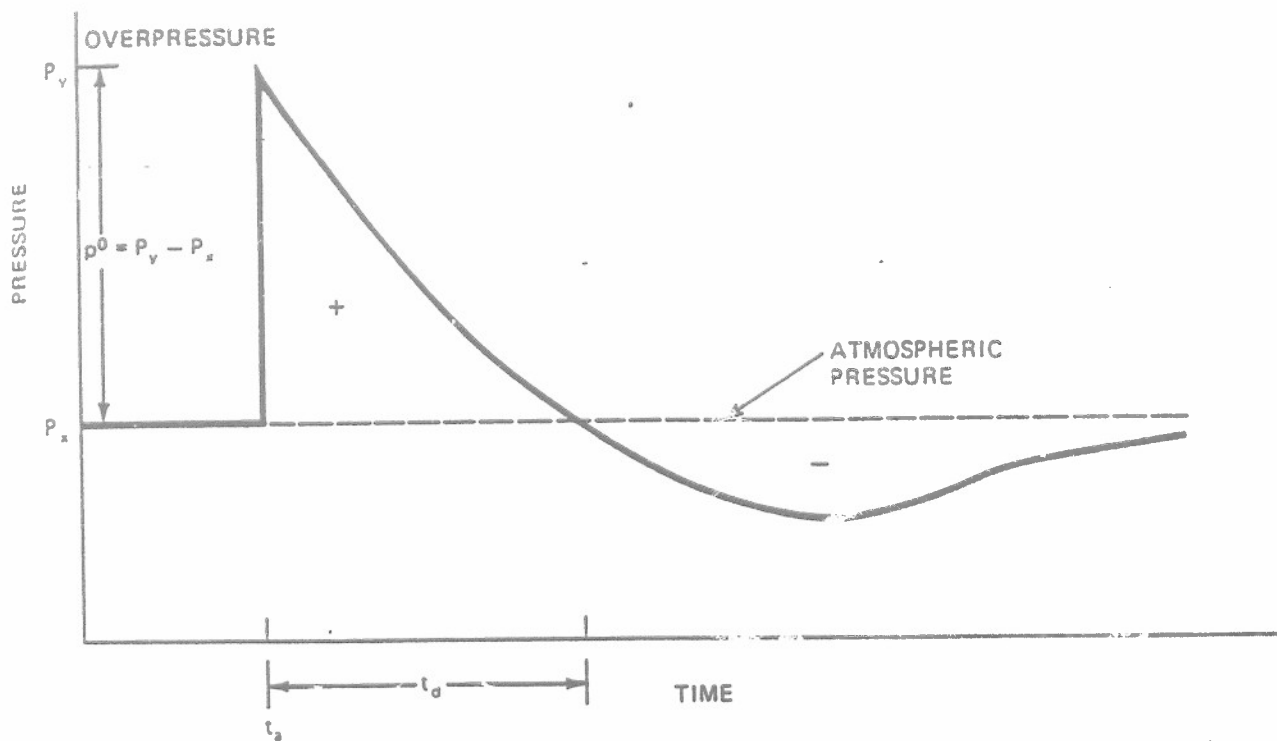


Figure 1 Typical pressure-time curve for an explosive blast wave.

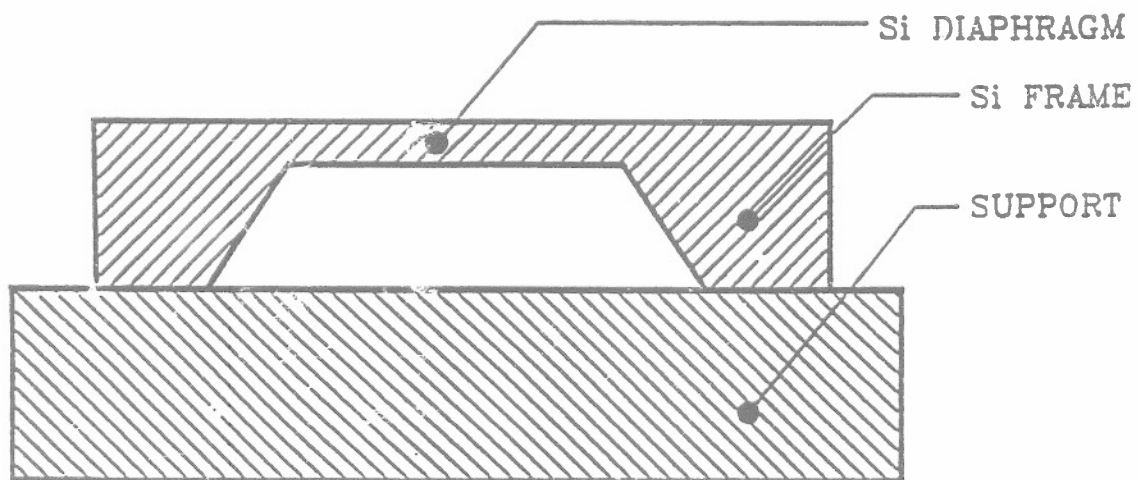


Figure 2 Silicon Diaphragm Supported by an Anisotropically Etched Frame

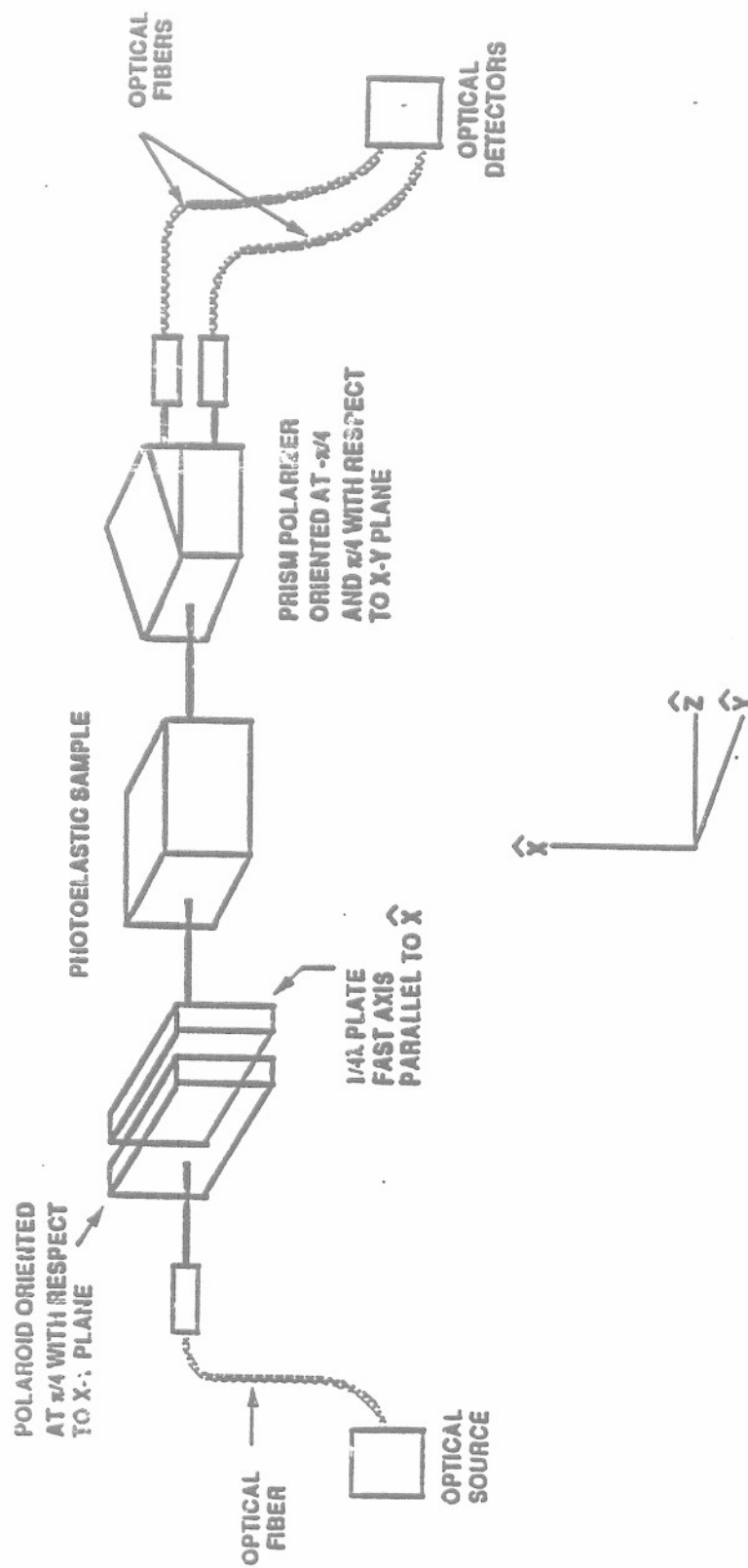


Figure 3. Schematic of the Optical Configuration of a Photoelastic Pressure Sensor

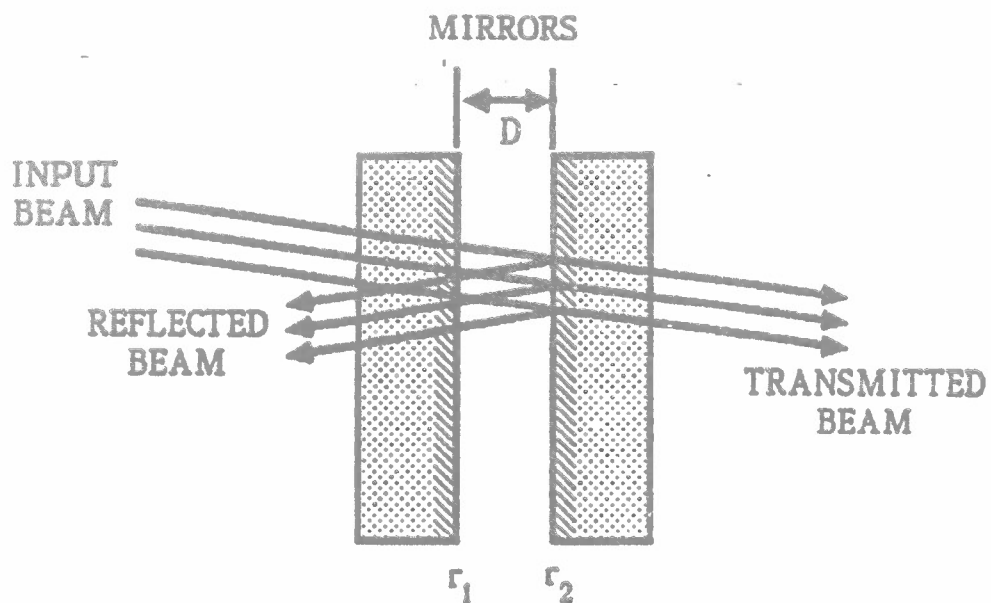


Figure 4 Schematic of a Fabry-Perot Optical Resonator

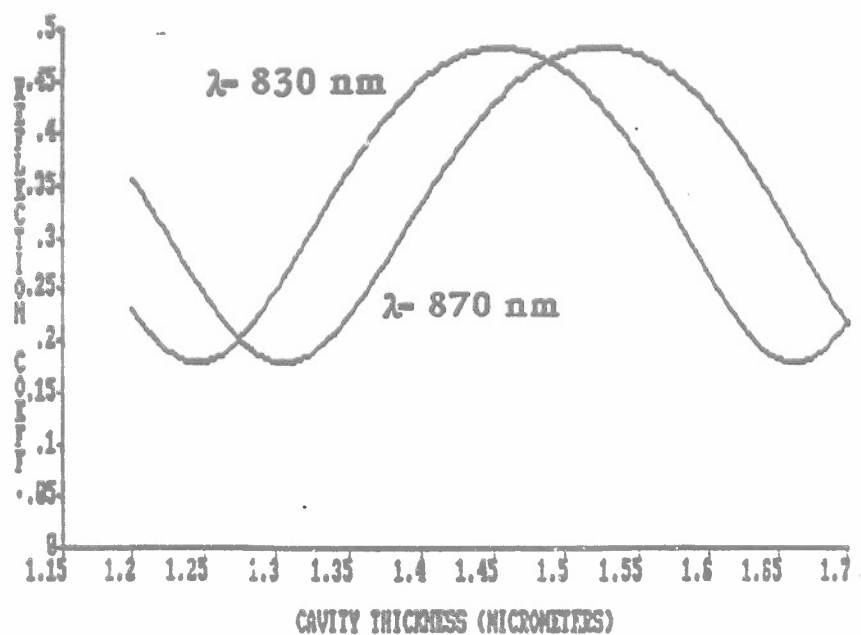


Figure 5 Reflectivity as a Function of Thickness, with Wavelength as a Parameter

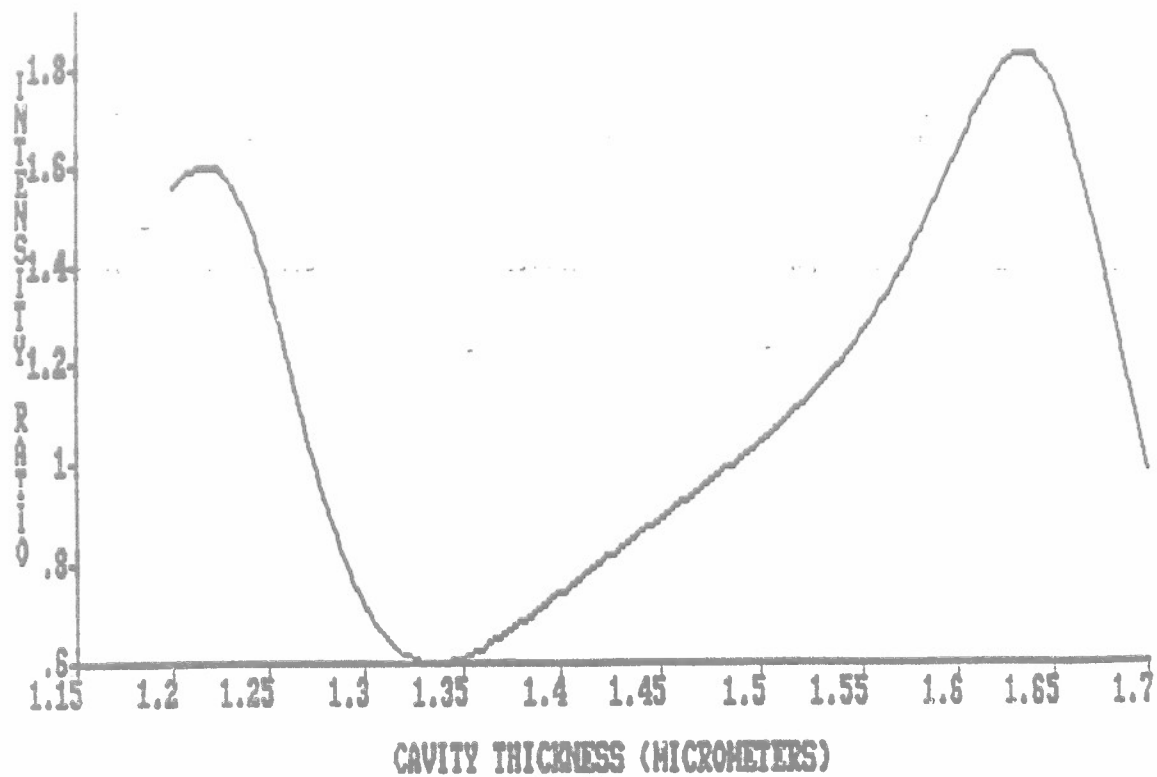


Figure 6 The Ratio of the Two Channels, as a Function of Resonator Thickness

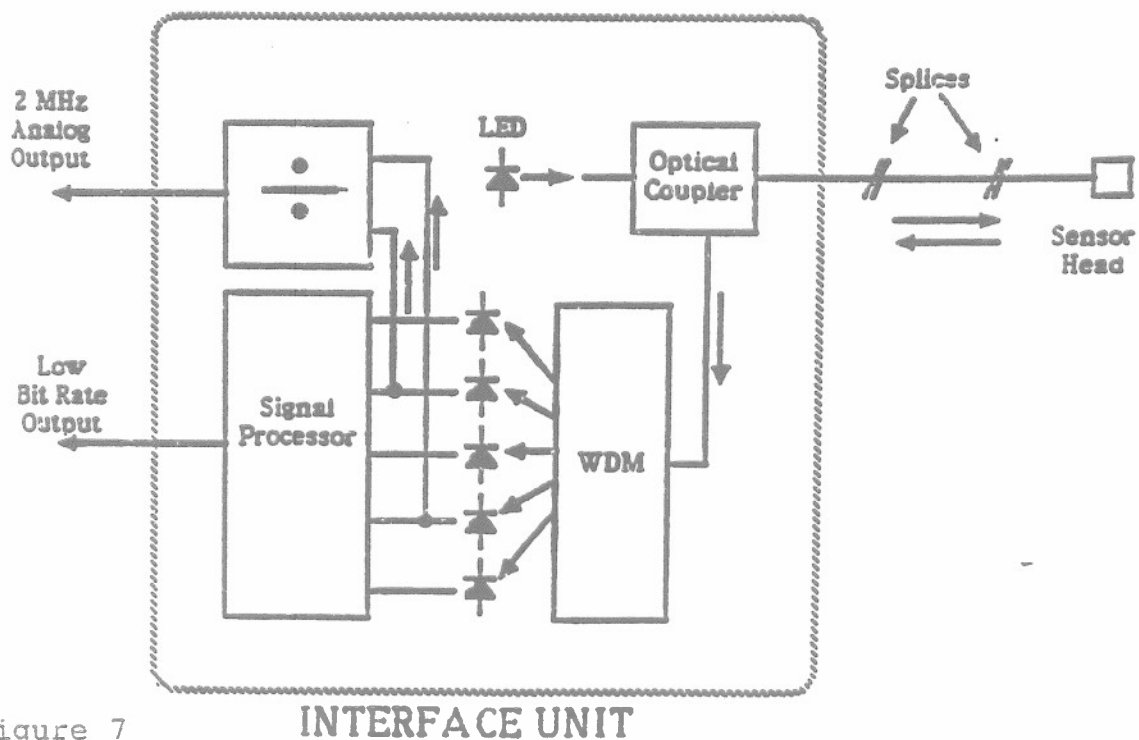


Figure 7

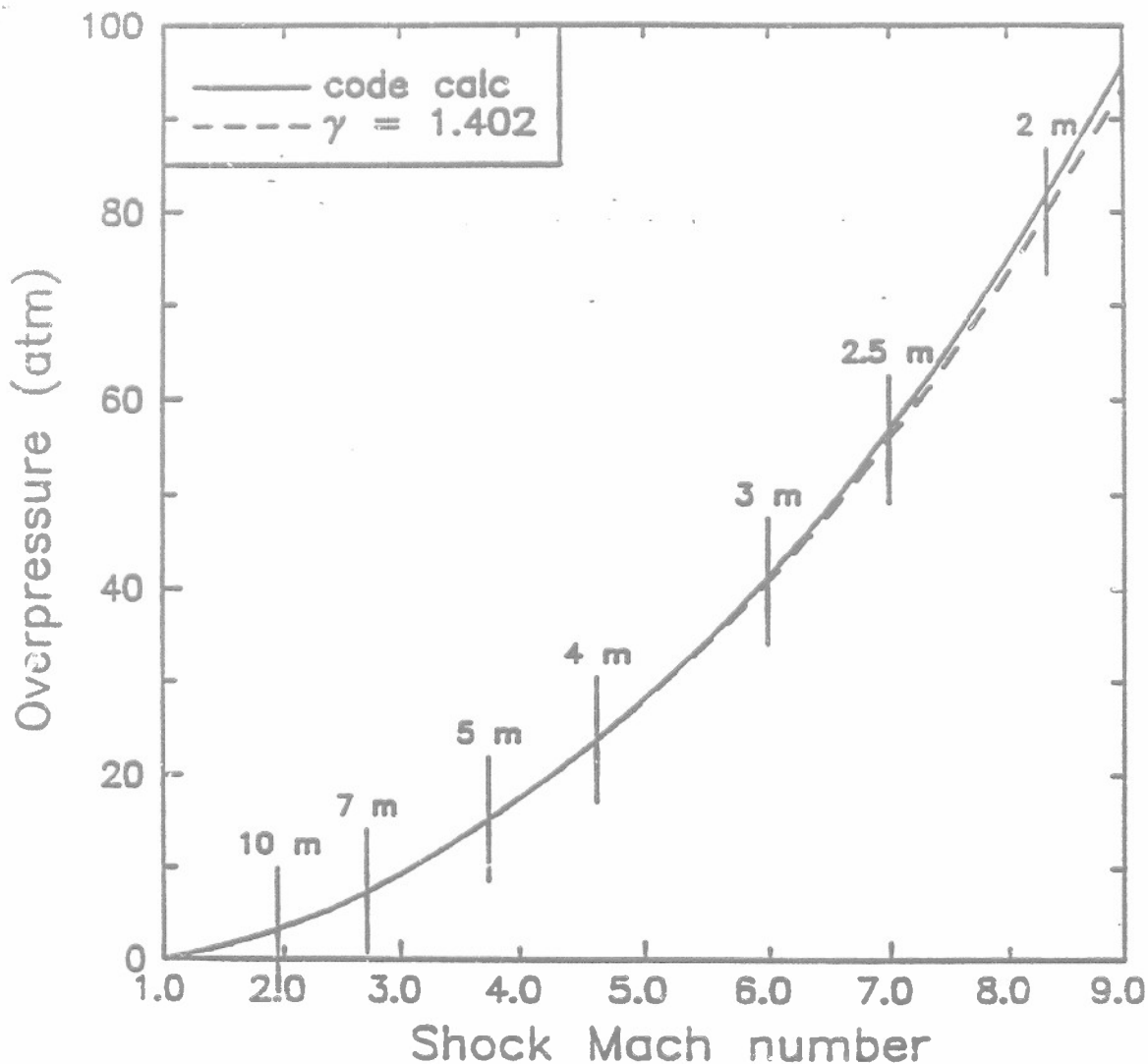


Figure 8. Calculated Relationship Between the Shock Speed and the Peak Pressure of the Shock

The solid line is obtained with a detailed computer code calculation, including molecular dissociation effects. The dashed line is a simple ideal gas calculation with $\gamma = 1.402$. The curves are practically indistinguishable below Mach 6. The curves are marked with the distances from a 500-pound explosion at which various shock speeds are expected. Beyond 3 meters from the model explosion the shock speed is Mach 6 or less, and the ideal gas approximation for deducing the peak pressure from the shock speed yields accurate results.